

# SUBSIDENCE AND HEAT PROPAGATION MODELING ON THE UNDERGROUND COAL GASIFICATION (CASE STUDY AT MUARA ENIM FORMATION, SOUTH SUMATERA)

## PEMODELAN PENURUNAN TANAH DAN RAMBATAN PANAS PADA GASIFIKASI BATUBARA BAWAH TANAH (STUDI KASUS DI FORMASI MUARA ENIM, SUMATERA SELATAN)

ZULFAHMI<sup>a</sup>, ILDREM SYAFRI<sup>b</sup>, ABDURROKHIM<sup>b</sup> and RIDHO K. WATTIMENA<sup>c</sup>

<sup>a</sup> R & D Center for Mineral and Coal Technology

Jl. Jend. Sudirman No. 623 Bandung 40211

e-mail: [zulfahmi.1966@esdm.go.id](mailto:zulfahmi.1966@esdm.go.id)

<sup>b</sup> Faculty of Geology Engineering-Padjadjaran University

<sup>c</sup> Faculty of Mining and Petroleum Engineering-ITB

### ABSTRACT

One of the important issues to study underground coal gasification (UCG) is the prediction of surface subsidence. Several parameters that influence these conditions are the thickness of cap rock, the physical and mechanical characteristics, the structure condition, the minerals composition of the rock, and external conditions. This study had been carried out simulation and modeling to determine the level of surface subsidence risk and the effect of high temperatures due to the activities. The modeling results show that the thickness of the rock above the UCG coal seam greatly affects the surface subsidence. The depth is more than 200 m and found that the SF value is 1.59 which indicates UCG reactor depth of  $\geq 200$  m is safe from the risk of subsidence. From the characteristic aspect of the cap rock, the claystone types which not contain kaolinite minerals are more prone to collapse than those of contain kaolinite minerals. From this models, the gasifier at 150 m depth was estimated that there will be a decline of -7.23 m, and the minimum subsidence is at 275 m about 0.1 m. The heat propagation modeling results show that at 50 m the temperature is estimated to be 213- 289°C, but if the thickness of the cap rock is > 200 m depth, the temperature is around 29-28°C.

Keywords: numerical modeling, subsidence, cap rock, kaolinite, non-kaolinite.

### ABSTRAK

Salah satu isu penting yang perlu dikaji dalam kegiatan gasifikasi batubara bawah tanah (UCG) adalah prediksi penurunan permukaan. Beberapa parameter yang memengaruhi kondisi tersebut adalah ketebalan batuan penutup, sifat fisik dan mekanik, kondisi struktur dan komposisi mineral batuan serta kondisi eksternal. Pada penelitian ini telah dilakukan simulasi dan pemodelan untuk mengetahui tingkat risiko penurunan muka tanah dan pengaruh suhu tinggi akibat aktivitas tersebut. Hasil pemodelan menunjukkan bahwa ketebalan batuan di atas lapisan batubara UCG sangat memengaruhi penurunan permukaan. Kedalaman lebih dari 200 m didapatkan nilai SF 1,59 yang menandakan kedalaman reaktor UCG  $\geq 200$  m aman dari resiko subsidence. Dari aspek karakteristik batuan penutup, jenis batulempung yang tidak mengandung mineral kaolinit lebih rentan mengalami keruntuhan dibandingkan dengan yang mengandung mineral kaolinit. Dari model ini, gasifier pada kedalaman 150 m diperkirakan akan terjadi penurunan sebesar -7,23 m, dan penurunan minimum pada 275 m sekitar 0,1 m. Hasil pemodelan perambatan panas menunjukkan bahwa pada kedalaman 50 m diperkirakan temperatur 213-289°C, namun jika ketebalan batuan penutup pada kedalaman > 200 m maka suhu sekitar 29-28°C.

Kata kunci: pemodelan numerik, penurunan permukaan tanah, batuan penutup, kaolinit, non-kaolinit.

**INTRODUCTION**

Based on the preliminary study, Indonesia has potential resources in four coal basins which can be developed using underground coal gasification (Purnama and Huda, 2019). The estimated resources at the four basins are 1,662.7 MT and the hypothetical gas resources total of 8.38 TSCF (Purnama and Huda, 2019). The exploited coal would become uneconomical resources if mined conventionally rather than using the UCG technology. This technology offers a cleaner, safer and cheaper method. However, it has several potential risk that should be anticipated. One of them is the surface subsidence. This condition will also cause disturbance the continuity of the UCG process.

The cap rock or rock around the coal seam will change the UCG process due to the cavity occurrence and thermal load. The failure may occur around the gasifier if the rock around the gasifier cannot withstand the thermal load, rock mass and hydrostatic pressure. If the failure occur and the roof rock or rock around the gasifier leaked then several possibilities, such as damage of the injection or production well, aquifer contamination, loss of heat energy and surface subsidence will occur.

It is important to be aware of the surface subsidence because it involves the possibility of environmental problems on the surface, such as the vital structures standing at the zone of the ground subsidence, and the environmental problems on the subsurface due to outflow of the harmful contaminants from the UCG cavities to the groundwater layer (Gregg, 1977; Sury *et al.*, 2004; Walter, 2007).

This study aims to predict the level of surface subsidence and heat propagation on the location of UCG. The study had designed a simulation and numerical modeling based on the laboratory test data such as the physical and mechanical value of rock and coal. All primary data were taken from Muara Enim Formation, South Sumatera Basin located at Macang Sakti Village, Musi Banyuasin Regency of South Sumatera Indonesia. Some secondary data are also used and were taken from a literature.

**METHOD**

This research is based on simulation and modelling using the main data of the rock samples characteristics from the study location. The type of rocks used are claystone, siltstone, sandstone, and coal as the base for the laboratory test. After core preparations, the samples were tested in the geomechanics laboratory before and after a thermal treatment. The results of the laboratory test are inserted into the software. The finite element software is used for modelling and calculation. The software is Ansys (version 17&18) where each command used to form this model is stored in the input file. The basis for calculating the model in this study is the criteria of failure with the conditions before and after being given thermal load to the rock samples. The characteristics of the rock after being given a thermal load can weaken or harden depending on the mineral composition contained in the rock (Zulfahmi *et al.*, 2017a).

According to Tian *et al.* (2016), the rock failure for the thermo-mechanical conditions is highly dependent on the correlation of stress components, hardening parameters and thermal loads. This condition describes the ultimate strength of the material under complex conditions, multi-axial stress conditions, complicated hardening, or weakening conditions that need to be explained by the internal variables such as mineral composition that will be changed due to the thermal loads (Zulfahmi *et al.*, 2017b).

General formulation of the thermo-mechanical failure criteria can be defined by the following equation (Turteltaub, 2002; Neto, Peric and Owen, 2008; Szabó and Kossa, 2012; Tian *et al.*, 2016):

$$f(\sigma_{ij}, H_{\alpha}, T) = 0 \dots \dots \dots (1)$$

Where  $\sigma_{ij}$  is stress condition,  $H_{\alpha}$  is the hardening parameters and T is thermal load. As previously discussed, the strength of rocks varies with changes in thermal load.

The combination of Mohr-Coulomb, Von Mises and Drucker-Prager failure criteria in the modeling using Ansys software are the basis for calculations carried out in this study because it involves materials that have a complex composition with the thermal loading treatments.

**Mohr-Coulomb Criterion**

The Mohr-Coulomb failure criterion is better known for its ease of mathematical formulation. The Mohr envelope is considered a straight line and the equation is expressed as the Mohr-Coulomb criterion by the equation:

$$\tau = C + \mu \sigma \dots\dots\dots(2)$$

Where  $\tau$  is shear stress,  $\sigma$  is normal stress,  $C$  is cohesion and  $\mu$  is internal friction angle on the rock or  $\tan \phi$ . The Mohr-Coulomb (MC) failure criterion can be expressed using the terminology of major and minor principal stresses as described in Equation 3.

$$\sigma_1 = \sigma_3 \frac{1 + \sin \phi}{1 - \sin \phi} + \frac{2c \cos \phi}{1 - \sin \phi} \dots\dots\dots(3)$$

Where the  $\sigma_1$  and  $\sigma_3$  respectively show the value of major and minor principal stresses,  $c$  is cohesion and  $\phi$  is inner friction angle. The linear regression analysis traditionally used to determine the strength parameters of  $c$  and  $\phi$ , and generally produced very good results. To predict the UCS value ( $\sigma_c$ ) through Equation 1 is given in Equation 4.

$$\sigma_c = \frac{2c \cos \phi}{1 - \sin \phi} \dots\dots\dots(4)$$

**Von Mises Criterion**

The single failure theory often is not always applicable to some of the materials analyzed. The von Mises criterion provides a realistic estimate of failure, which is often known as the maximum distortion energy criterion, the octahedral shear stress theory, or the Maxwell-Huber-Hencky-von Mises theory, often used to estimate ductile materials (Christensen, 2019). The von Mises stress distribution under tensile or compressive conditions can also be used as a criterion for understanding the failure mechanism (Sica, 2017). The von Mises criterion defines that a failure occurs when the distortion energy reaches energy equal to the yield energy or failure ( $\sigma_y$ ) at the uniaxial stress. Mathematically, expressed by Equation 5.

$$\frac{1}{2} [(\sigma_1 - \sigma_2)^2 + (\sigma_2 - \sigma_3)^2 + (\sigma_3 - \sigma_1)^2] \leq \sigma_y^2 \dots\dots\dots(5)$$

This equation represents an elliptical shape of the principal stress as described in Figure 1.

**Drucker-Prager Criterion**

The Drucker-Prager yield criterion is a simple modification of the von Mises criterion, in which the hydrostatic stress component is also included to introduce pressure-sensitivity (Drucker and Prager, 1952). The Drucker and Prager failure criterion is a generalization of the Mohr-Coulomb failure criterion and isotropic yield conditions. The Drucker-Prager plasticity model differs from the conventional metal plasticity model because of its dependence on hydrostatic pressure. For a linear yield surface (the term linear refers to the linear shape when plotted on the field of effective stress versus hydrostatic pressure) indicates that the value of the hydrostatic stress, the yield strength will be smaller.

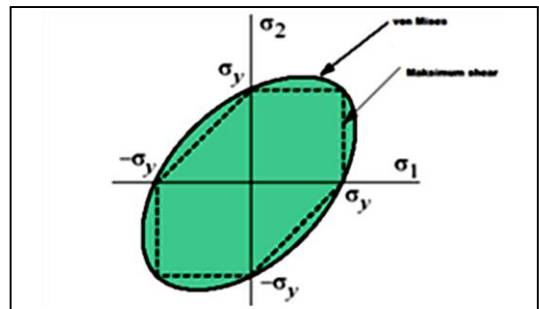


Figure 1. The illustration of von Mises criteria (Pilkey, 1994)

Conversely, when hydrostatic compression increases, it will result in high yield strength. When the yield surface is plotted in the main stress space, it will look like a cone (Figure 2). The two main characteristics found are that (a) a change in yield strength depending on the state of the hydrostatic stress and (b) some inelastic volumetric strain can occur, as defined by the flow potential. In the Ansys software there are three supported the models that is Drucker - Prager the Extended Drucker - Prager and the Drucker - Prager Cap model.

For some of the current geomechanical analyses, the extended Drucker - Prager model is widely used as complements to the shortcomings of the Drucker - Prager model, namely the use of perfect plastic behavior and the linear yield surface requirements. The strain hardening behavior is determined by adding an isotropic hardening plasticity

model to the material identification (such as rock hardening).

$$c = \frac{3^{1/2} \sigma_y (3 - \sin(\phi))}{6 \cos(\phi)} \pi r^2 \dots \dots \dots (9)$$

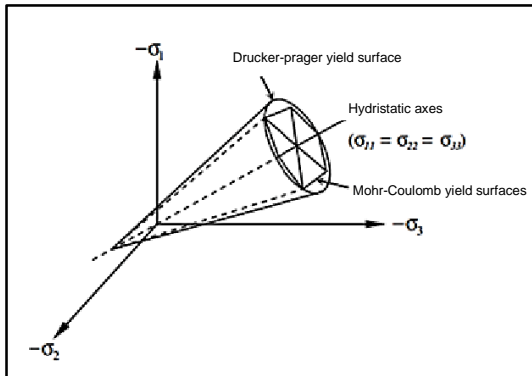


Figure 2. Drucker-Prager and Mohr-Coulomb yield surface models

To simulate the effect of a cracked surface on the model, Ansys uses the concept of contact and target surface development. This is mainly done to determine the presence of fractures. The next section discuss a description of the contact and target elements used to simulate the required requirements. According to Li and Liu (2000) in Boldyrev and Muzemnek (2008), the equation of a yield surface in Druker-Prager model is:

$$F = S_h + 3\beta\sigma_m - \sigma_y = 0 \dots \dots \dots (6)$$

The  $S_h$  value is the intensity of shear stress;  $\sigma_m$  is the average stress at the points;  $\beta$  and  $\sigma_y$  are the parameters of the model. If the model allow to determine two points laying on a yield surface for example  $(\sigma_{m1}, S_{h1})$  and  $(\sigma_{m2}, S_{h2})$ , by substitution, it can be have the equation as (Boldyrev and Muzemnek, 2008):

$$\sigma_y = S_{h1} + 3\beta\sigma_{m1}; \beta = \frac{1}{3} \frac{S_{h2} - S_{h1}}{\sigma_{m2} - \sigma_{m1}} \dots \dots \dots (7)$$

If the parameters are correlated with Mohr-Coulomb parameters, it will be had the equation Boldyrev and Muzemnek (2008):

$$\sigma_y = \frac{6c \cos(\phi)}{3^{1/2} (3 - \sin(\phi))}; \beta = \frac{2 \sin(\phi)}{\sqrt{3} (3 - \sin(\phi))} \dots \dots \dots (8)$$

The  $c$  value is the cohesion and  $\phi$  is the angle of internal friction. In the other way, the cohesion can be determined from the equation (Boldyrev and Muzemnek, 2008):

**RESULTS AND DISCUSSION**

One of the important considerations in the UCG activities is the possibility of surface subsidence around the location. Ellison and Schubert (1981); Whittaker and Reddish (1989); Waddington and Kay (1995); Asadi *et al.* (2005) have conducted the research on the effects and potential of surface subsidence as well as calculations of its magnitude of subsidence decrease. They used graphics and mathematical models to interpret the decrease of subsidence. The surface subsidence of the UCG generally refers to the experience in the underground coal mining (UCM). The result observations presented by researchers such as Huayang *et al.* (2002); Zangerl (2003); Asadi *et al.* (2005) are very helpful in illustrating a model of subsidence in the UCG process. Therefore, the treatment of the cavity conditions from the gasification process is almost the same as UCM, however, the thermal effect is an important concern in determining the dimensions of the pillars. The subsidence profile of the flat and dip coal seam is shown in Figure 3.

After the rapid development in computing technology, a numerical modeling has been widely used to predict land subsidence, both for UCM calculations (Dyne, 1998; Sroka, Tajdus and Preusse, 2011; Dong *et al.*, 2013; Seccombe, 2014) and calculations for UCG (Tian, 2013; Sirdesai *et al.*, 2015; Tian *et al.*, 2016). The UCG generally uses numerical modeling based on a finite element or finite difference methods. Both models have been introduced since 1980 by Langland and Trent (1981) who predicted the ground subsidence at Hoe Creek, Wyoming and concluded that the thermal effect greatly affected the rock strength conditions around the gasifier. The boundary model and finite element analysis for thermo-elasto-plastic and thermo-visco-elastic recommended by Advani *et al.* (1983) can be used to evaluate the sensitivity of some parameters that determine the span of cavity forms, roof failure, ground subsidence, pore pressure, and creep. Lee *et al.* (1985, 1986) have accomplished a series of numerical experiments to provide guidance on finite element modeling for predicting ground subsidence due to the UCG process

and proposed that in the interactions between in situ stresses and cavities are being the most dominant factor on the evaluation of subsidence. Meanwhile, Siriwardane, Layne and Martin (1989) thought that the geological conditions and the mechanical properties of rocks could directly have a significant influence on the UCG process and the magnitude of the deformations. However, ground subsidence caused by the UCG process on the commercial scale is not identifiable until now.

### Geometry and Boundary Conditions

In this paper, the modeling and completion of the calculation using the finite element software. The software is Ansys where each command used to form this model is stored in the input file. The shape of the model is a rectangular block that consists rock layers

around the coal seam and is affected by heat due to gasification process. Data on the physical and mechanical properties of rocks were obtained from the result of laboratory test. Some secondary data from literature studies are also used to complement the modeling. This modeling uses a static structural assumption that the material and thermal conditions are elastic isotropy. To simplify the form of 3D modeling, the variation of lithology of 24 rock layers above the coal seam target is simplified into five different rock characteristics and one coal seam with 9-10m thickness. The five rock types are distinguished based on their composition of mineral content, RC1 and RS1 consecutive are claystone and siltstone that is predominantly kaolinite, RC2 and RS2 consecutive are claystone and siltstone that are not predominantly kaolinite and RSS2 is sandstone.

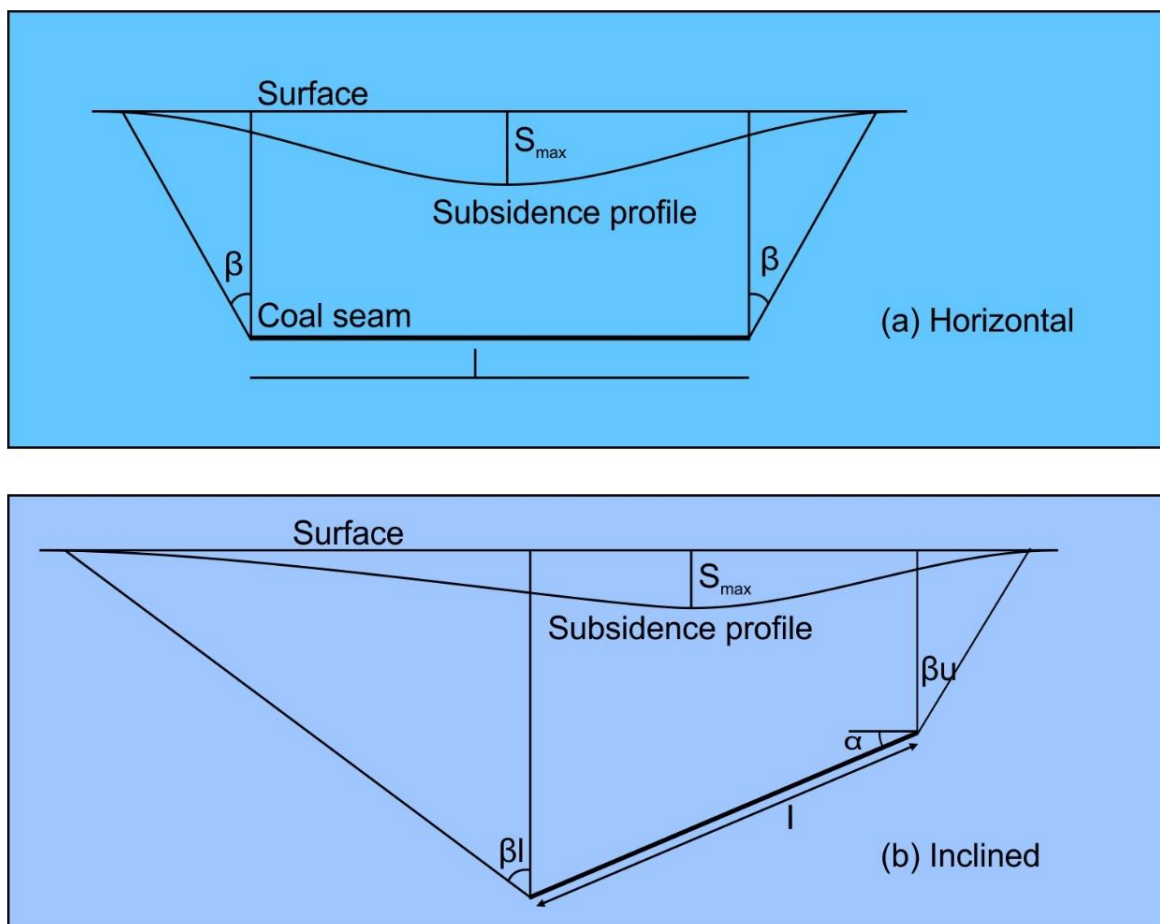


Figure 3. Subsidence profile on the flat and dip coal seam (Asadi *et al.*, 2005)

The dimensions model of the UCG location is 500 m x 500 m x depth (m). The simulated target coal seam depth varies to a depth of 275 m. The boundary condition of the model for the lower plane is considered fixed (fixed support), while the vertical side is considered able to move freely vertically but cannot move horizontally (frictionless support). The numerical model made is considered to have occurred cavities due to the gasification process with dimensions of length, width and height of 100 m x 100 m x 9 m. The application of a structured mesh allows for the appropriate repair of the network to maintain numerical accuracy around the UCG gasifier. Figure 4 shows the dimensions and boundary conditions of the used model. The stress boundary condition above the rock layer around the target coal seam is considered a vertical stress ( $\sigma_v$ ) in which the magnitude is adjusted to the depth of the rock layer from the surface. While the horizontal stress ( $\sigma_h$ ) is influenced by the geotectonic loads in the form of earthquake factors. Based on the results of the probabilistic analysis researched by Irsyam *et al.* (2010) for six earthquake scenarios in Indonesia, it shows that even if the research is in disaster zone for earthquake, the probability retained low ranging from 0.05 g to 0.1 g.

**The Rock and Coal Characteristics**

The results of the research shows that the properties of rocks are very dependent on the temperature. The difference in these characteristics is not only for the type of rock, but also the mineral content that forms the rock itself (Zulfahmi *et al.*, 2017b). In line with several literature reviews and studies that

have been conducted by Tian *et al.* (2009, 2012, 2016), Tian, Ziegler and Kempka (2011, 2014) and Tian (2013), it is concluded that the physical and mechanical properties of rocks are generally very dependent on temperature, and dependence on temperature varies for each rock type and initial conditions such as the presence of fissures (fine cracks) and structure and rate of heating. Rock thermal characteristics data such as linear thermal expansion coefficient, specific heat capacity and thermal conductivity for each rock being modeled are based on reviews conducted by several researchers such as Min, (1983), Tian (2013), Eppelbaum, Kutasov and Pilchin (2014) and Otto and Kempka (2015). While the physical, mechanical, and rock dynamic properties data were obtained from the author own research. Temperature conditions are adjusted to the tests room temperature (30°C) to 1100°C.

The physical and mechanical properties data of the rock were measured when it was already burned or in cold condition. This condition is adjusted with the assumption that the rock around the gasifier will experience maximum load during the cavity when the coal has burned. All data used in this modeling have been prepared and arranged as shown in Tables 1 to 6. By carrying out several simulations of the variation in the thickness of the rock around the coal target, it shows that the amount of surface subsidence will occur at the research location. These parameters are accommodated in the Ansys database, namely in the Engineering Data menu, as in Figure 5.

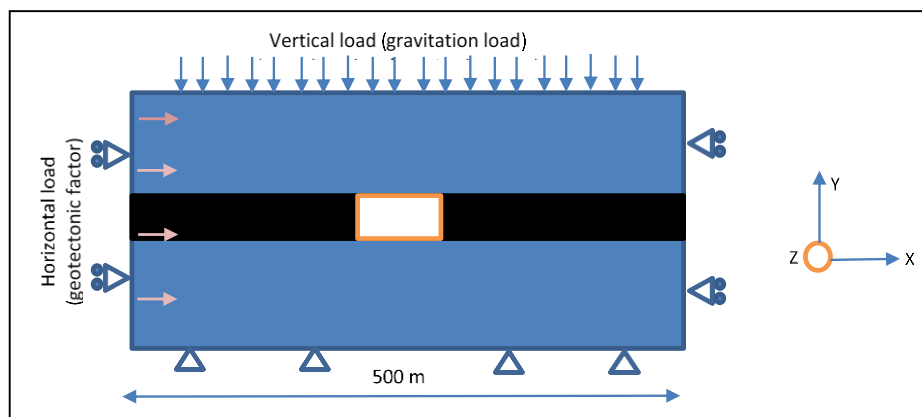


Figure 4. Dimension and boundary condition model

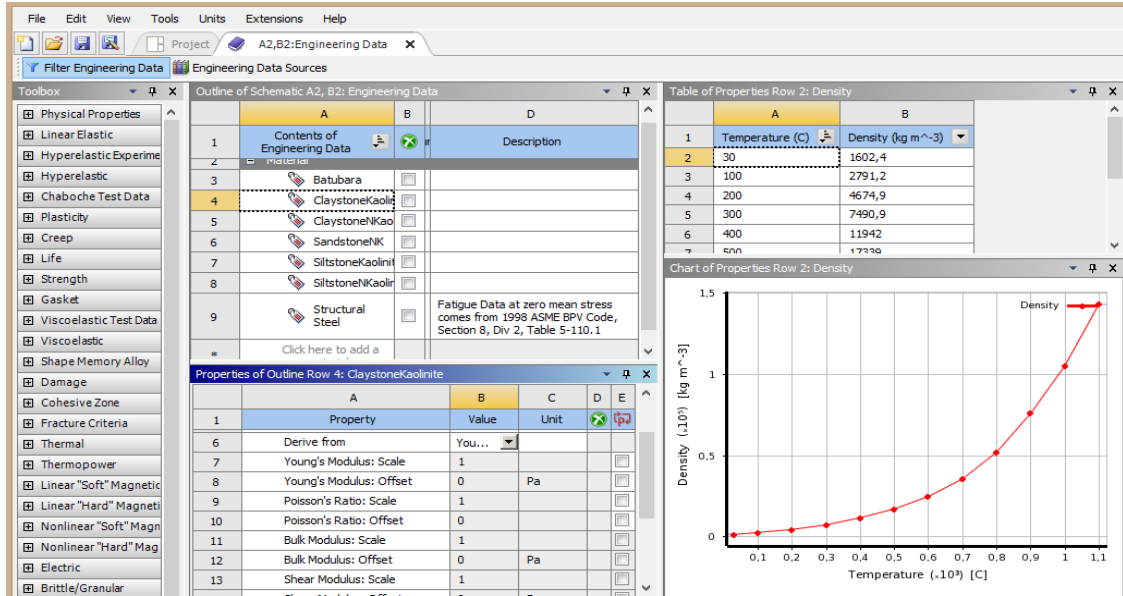


Figure 5. Rock and coal characteristic database

Table 1. Geomechanics and thermal properties of RC1

Temp. (°C)	Density (gr/cm <sup>3</sup> )	Modulus of Elasticity (kg/cm <sup>2</sup> )	Poisson Ratio	Others Characteristics
30	1.6024	5349.39	0.31	Tensile Strength (Pa) : 523184.78
100	1.7419	6655.38	0.42	Shear stress (Pa) : 36382.67
200	1.6748	5432.22	0.37	Compressive (Pa) : 3215600.53
300	1.6024	4368.68	0.25	$\alpha$ (/°C) : 3.13E-05
400	1.5942	2949.38	0.17	Cp (J/kg °C) : 2.13E-03
500	1.4520	11296.29	0.3	$\lambda$ (W/m/°C) : 1.42
600	1.4444	4442.63	0.26	
700	1.4292	3039.69	0.18	
800	1.4637	5246.6	0.31	
900	1.4558	12861.68	0.24	
1000	1.3835	26704.90	0.12	
1100	1.3593	16857.46	0.22	

Table 2. Geomechanics and thermal properties of RC2

Temp. (°C)	Density (gr/cm <sup>3</sup> )	Modulus of Elasticity (Kg/cm <sup>2</sup> )	Poisson Ratio	Others Characteristics
30	1.5583	6554.32	0.40	Tensile Strength (Pa) : 456401.49
100	1.5481	3917.71	0.23	Shear stress (Pa) : 31675.48
200	1.4538	4451.51	0.26	Compressive (Pa) : 3356816.30
300	1.6575	4868.34	0.25	$\alpha$ (/°C) : 3.13E-05
400	1.4744	1824.50	0.11	Cp (J/kg °C) : 2.13E-03
500	1.5108	3038.46	0.19	$\lambda$ (W/m/°C) : 1.42
600	1.6545	9864.32	0.29	
700	1.4871	8748.34	0.27	
800	1.5199	3049.23	0.21	
900	1.4554	1409.30	0.28	
1000	1.3987	3049.24	0.19	
1100	1.5674	1755.19	0.11	

Table 3. Geomechanics and thermal properties of RS1

Temp. (°C)	Density (gr/cm <sup>3</sup> )	Modulus of Elasticity (Kg/cm <sup>2</sup> )	Poisson Ratio	Others Characteristics
30	1.6736	1294.80	0.18	Tensile Strength (Pa) : 344801.81
100	1.6754	1411.34	0.19	Shear stress (Pa) : 32656.14
200	1.5776	3447.54	0.20	Compressive (Pa) : 2032526,28
300	1.6072	1475.39	0.20	$\alpha$ (/°C) : 2.13E-05
400	1.6029	12186.29	0.28	Cp (J/kg °C) : 7.95E-04
500	1.4849	7820.01	0.18	$\lambda$ (W/m/°C) : 2.22
600	1.5667	3933.07	0.22	
700	1.5317	4987.34	0.26	
800	1.4391	5188.97	0.27	
900	1.5172	23814.00	0.11	
1000	1.5000	20130.08	0.09	
1100	1.4658	3121.45	0.18	

Table 4. Geomechanics and thermal properties of RS2

Temp. (°C)	Density (gr/cm <sup>3</sup> )	Modulus of Elasticity (Kg/cm <sup>2</sup> )	Poisson Ratio	Others Characteristics
30	1.7120	4928.00	0.29	Tensile Strength (Pa) : 336564.23
100	1.6248	3009.77	0.18	Shear stress (Pa) : 33538.74
200	1.6888	3594.33	0.21	Compressive (Pa) : 2191295.94
300	1.6447	9757.02	0.19	$\alpha$ (/°C) : 2.13E-05
400	1.6403	1848.82	0.17	Cp (J/kg °C) : 7.95E-04
500	1.4892	2243.36	0.21	$\lambda$ (W/m/°C) : 2.22
600	1.6033	1071.58	0.10	
700	1.7242	1860.66	0.17	
800	1.4726	2454.05	0.23	
900	1.6458	1769.91	0.17	
1000	1.5350	1201.77	0.11	
1100	1.5182	1287.78	0.12	

Table 5. Geomechanics and thermal properties of RSS2

Temp. (°C)	Density (gr/cm <sup>3</sup> )	Modulus of Elasticity (Kg/cm <sup>2</sup> )	Poisson Ratio	Others Characteristics
30	1.6370	24774.39	0.38	Tensile Strength (Pa) : 573100.63
100	1.6550	20849.83	0.13	Shear stress (Pa) : 30204.48
200	1.4343	8685.41	0.13	Compressive (Pa) : 4259518.43
300	1.6387	17321.22	0.27	$\alpha$ (/°C) : 1,60E-05
400	1.6245	7843.25	0.12	Cp (J/kg °C) : 8,44E-04
500	1.7635	618.36	0.09	$\lambda$ (W/m/°C) : 1.55
600	1.6842	1223.96	0.23	
700	1.5448	697.91	0.16	
800	1.5172	1005.70	0.19	
900	1.5251	813.89	0.24	
1000	1.6387	1776.55	0.38	
1100	1.3777	1775.07	0.37	

Based on Table 1-5, it seems that the characteristics behavior of rocks after thermal load are non linier. That condition due to differences in its mineral composition of each tested rock sample, even if the type of tested sample in each variation of thermal treatment are the same. The differences of mineral content in these rocks can make the rock stronger or weaker when given a thermal

load. In addition, the difference in composition also causes differences in the release of hydroxyl groups in each rock sample, where at a certain temperature there is a release and an amorphous mass of alumina and silica is formed which makes the rock hardens and strengthens, but some are too fast causing the micro crack which makes the rock weaker.

**Structures Change of Rock Layers**

From the results of this modeling, the values of deformation (directional deformation, total deformation), stress and strain (normal stress, normal strain), stress and strain

distribution values and safety factor values were obtained in each model in 3D. Figures 6 to 11 illustrate the shape of the rock model around the UCG activity at each change in the layer thickness.

Table 6. Geomechanics and thermal properties of RSS2

Density	Kg/m <sup>3</sup>	1190.77
Modulus Elasticity	Pascal	644965473.40
Poisson Ratio	-	0.3613
Shear strength	Pascal	647238.90
Tensile stress	Pascal	374614.03
Compressive stress	Pascal	4015496.29
Linier thermal Expansion( $\alpha$ )	°C-1	0.000005
Specific Heat Capacity (Cp)	J/kg °C	2000
Thermal Conductivity	W/m°C	0.23

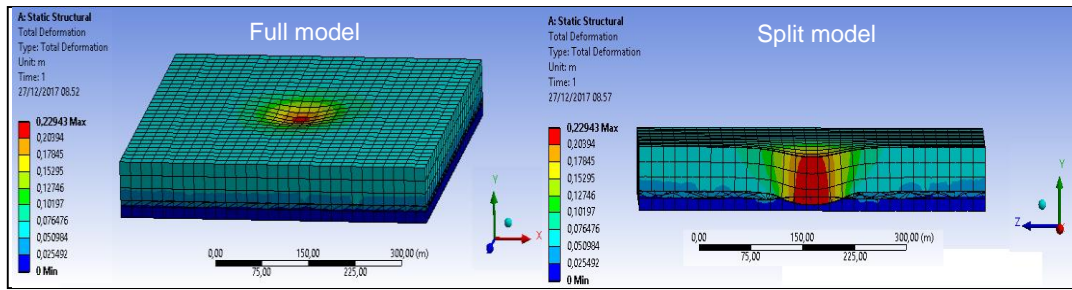


Figure 6. The model of rock around the UCG activity with 50 m thick

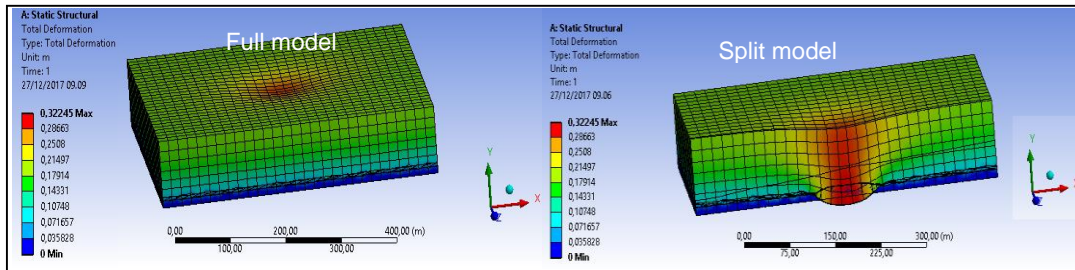


Figure 7. The model of rock around the UCG activity with 100 m thick

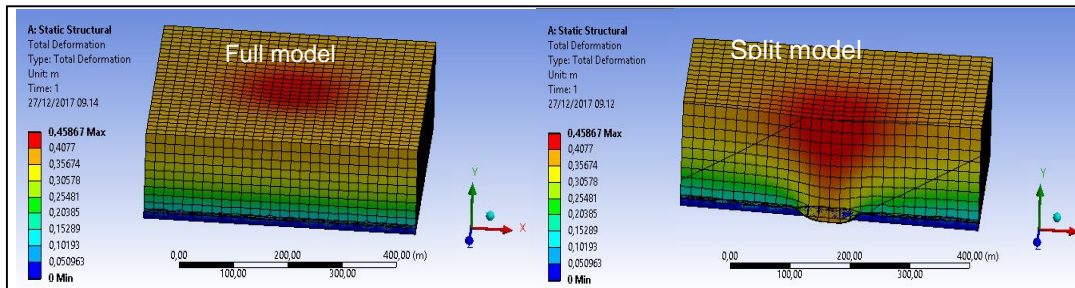


Figure 8. The model of rock around the UCG activity with 150 m thick

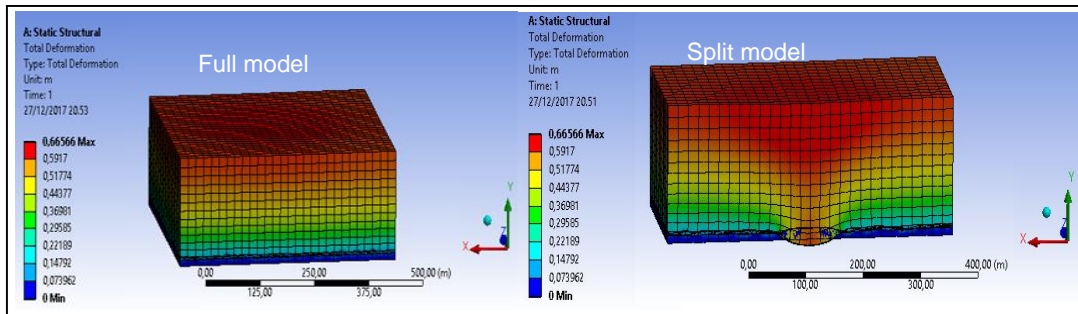


Figure 9. The model of rock around the UCG activity with 200 m thick

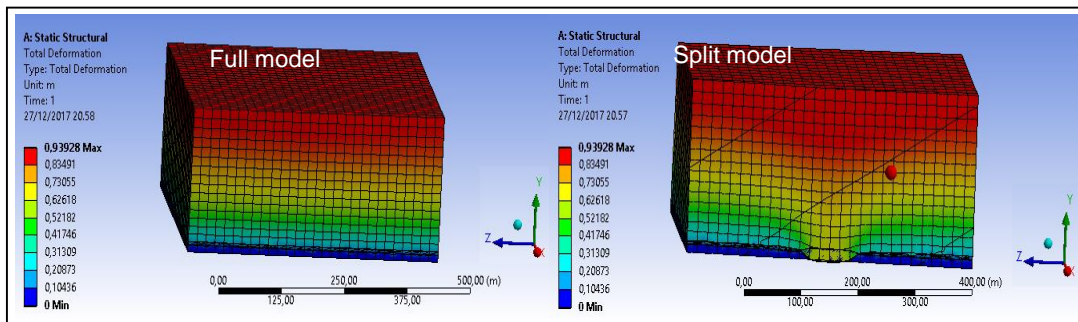


Figure 10. The model of rock around the UCG activity with 250 m thick

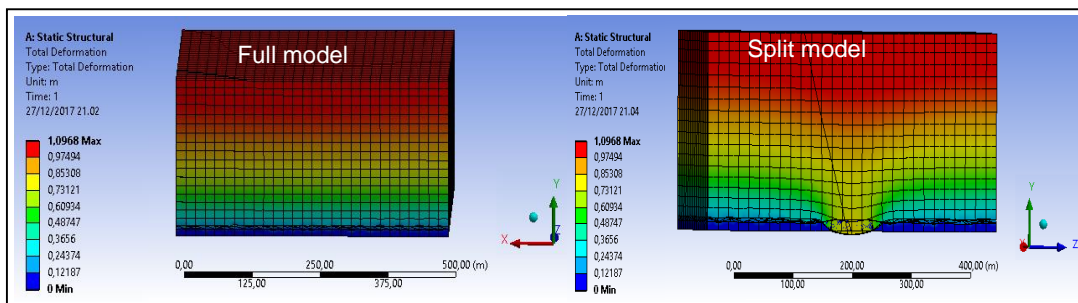


Figure 11. The model of rock around the UCG activity with 275 m thick

While the value of the safety factor in each model for each depth of 50, 100, 150, 200,

250 and 275 ms can be seen in Figures 12 to 14.

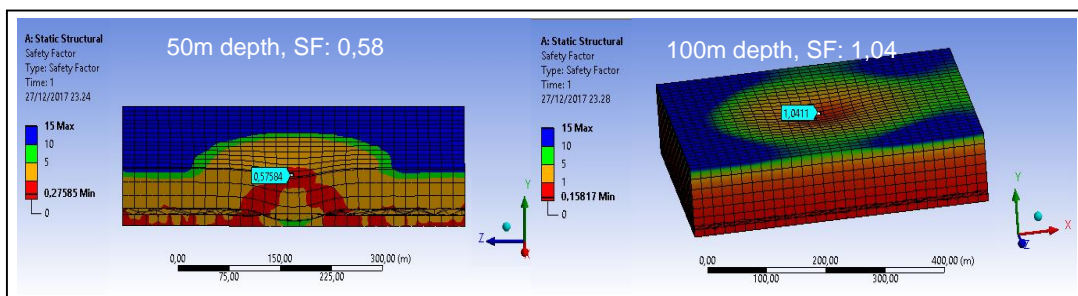


Figure 12. Safety Factor at 50 and 100 m depth

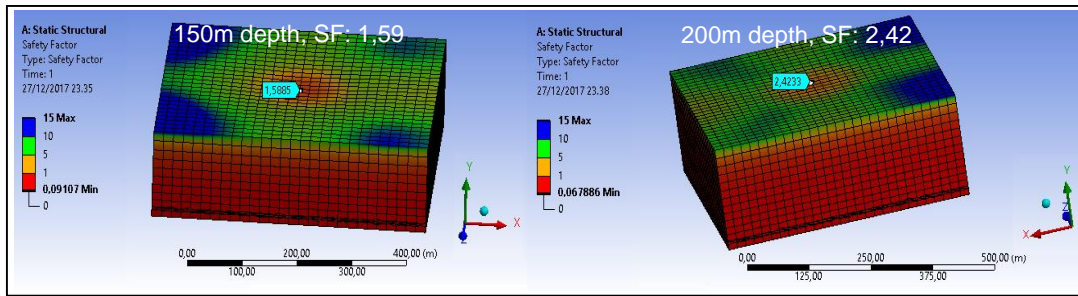


Figure 13. Safety Factor at 150 and 200 m depth

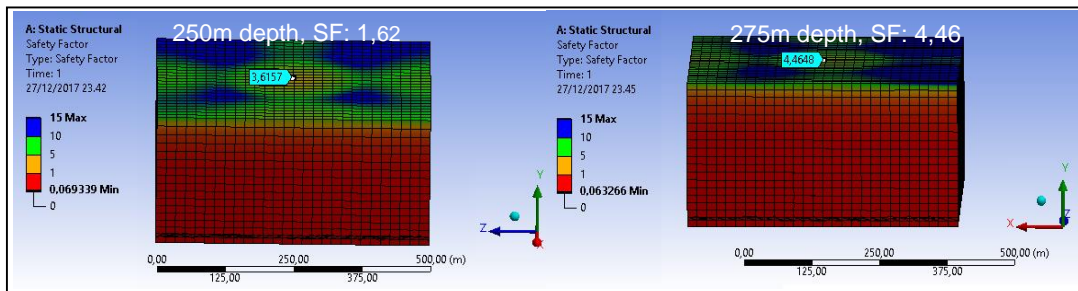


Figure 14. Safety Factor at 250 and 275 m depth

Table 7 is the summary of modelling result (total deformation, directional deformation, normal stress, normal strain and safety factor) at each depth.

Table 7. Summary of modelling result

Parameters	DEPTH (m)					
	50	100	150	200	250	275
<b>Claystone-RC1</b>						
Total deformation (m)	0.2290	0.3224	0.4590	0.6666	0.9393	1.0968
Directional def. (m)	0.0373	0.0244	0.0258	0.0335	0.0435	0.0437
Normal stress (Pa)	$7.73 \times 10^5$	$8.59 \times 10^5$	$1.09 \times 10^6$	$1.38 \times 10^6$	$1.69 \times 10^6$	$1.81 \times 10^6$
Normal strain (m)	0.001097	0.001499	0.00142	0.00181	0.00215	0.00228
Safety Factor	0.57	1.04	1.58	2.42	3.62	4.46
<b>Claystone-RC2</b>						
Total deformation (m)	0.1790	0.2460	0.3490	0.4520	0.5590	0.6350
Directional def. (m)	0.0290	0.020	0.027	0.037	0.047	0.053
Normal stress (Pa)	$7.01 \times 10^5$	$7.37 \times 10^5$	$7.47 \times 10^5$	$9.15 \times 10^5$	$1.10 \times 10^6$	$1.23 \times 10^6$
Normal strain (m)	0.00098	0.00158	0.00182	0.0024	0.00217	0.00258
Safety Factor	0.58	0.91	1.47	2.14	3.16	3.90
<b>Siltstone-RS1</b>						
Total deformation (m)	0.731	1.117	1.906	3.009	4.428	5.250
Directional def. (m)	0.118	0.082	0.108	0.143	0.179	0.149
Normal stress (Pa)	$5.26 \times 10^5$	$6.92 \times 10^5$	$1.10 \times 10^6$	$1.43 \times 10^6$	$1.77 \times 10^6$	$1.32 \times 10^6$
Normal strain (m)	0.00327	0.00413	0.00643	0.00834	0.0103	0.00758
Safety Factor	0.59	0.99	1.70	2.73	4.20	5.39
<b>Siltstone-RS2</b>						
Total deformation (m)	0.264	0.373	0.537	0.798	0.131	1.328
Directional def. (m)	0.043	0.028	0.033	0.043	0.053	0.053
Normal stress (Pa)	$8.61 \times 10^5$	$8.49 \times 10^5$	$1.22 \times 10^6$	$1.55 \times 10^6$	$1.90 \times 10^6$	$2.00 \times 10^6$
Normal strain (m)	0.00131	0.00163	0.00174	0.00221	0.00271	0.00291
Safety Factor	0.41	0.64	1.04	1.59	2.36	2.86
<b>Sandstone-RSS2</b>						
Total deformation (m)	0.078	0.106	0.147	0.191	0.240	0.273
Directional def. (m)	0.0160	0.0166	0.0217	0.0291	0.0365	0.0425
Normal stress (Pa)	$9.48 \times 10^5$	$9.98 \times 10^5$	$9.49 \times 10^5$	$1.15 \times 10^6$	$1.38 \times 10^6$	$1.49 \times 10^6$
Normal strain (m)	0.000959	0.000705	0.000461	0.000392	0.000478	0.000546
Safety Factor	0.45	0.77	1.16	1.90	2.54	3.17

To evaluate the stability of each rock type studied (RC1, RC2, RS1, RS2 and RSS2) to surface subsidence due to the loads it experienced during the UCG process, then on the model measures the amount of subsidence that occurs in each depth. Figure 15 is one of the rock types (RC1) that illustrated the magnitude of surface subsidence for 150 – 275 m depth.

Table 8 shows the complete surface subsidence value for each rock type at several depths. It can be seen that the maximum of surface subsidence occurs in RC2 (non-kaolinite claystone) with a decrease of 7.23 m if the UCG process is only 150 m from the surface. The minimum surface subsidence is only 10 cm for RC1 type (kaolinite claystone) with the depth of UCG process is 275 m from the surface.

The simulation of surface subsidence is only carried out at the thickness of the cap-rock

which has a value of SF > 1.3 (150 - 275 m depth). From these results, it shows that the surface subsidence will decrease along with the increase of the thickness of the cap-rock which functions as a protective gasifier in the UCG process. Meanwhile, when viewed from the rock type, rocks that have non-kaolinite (RC2, RS2, RSS2) will easily collapse compared to those containing kaolinite (RC1 and RS1).

**Thermal Propagation Model**

The thermal load model is carried out at a gasifier room temperature at around 1,100°C. Data on thermal conductivity, heat flow rate and other thermal parameters were entered in the program database listed in Table 6. Figure 16 to 18 shows a model of heat propagation from the heat source (gasifier) to the surface.

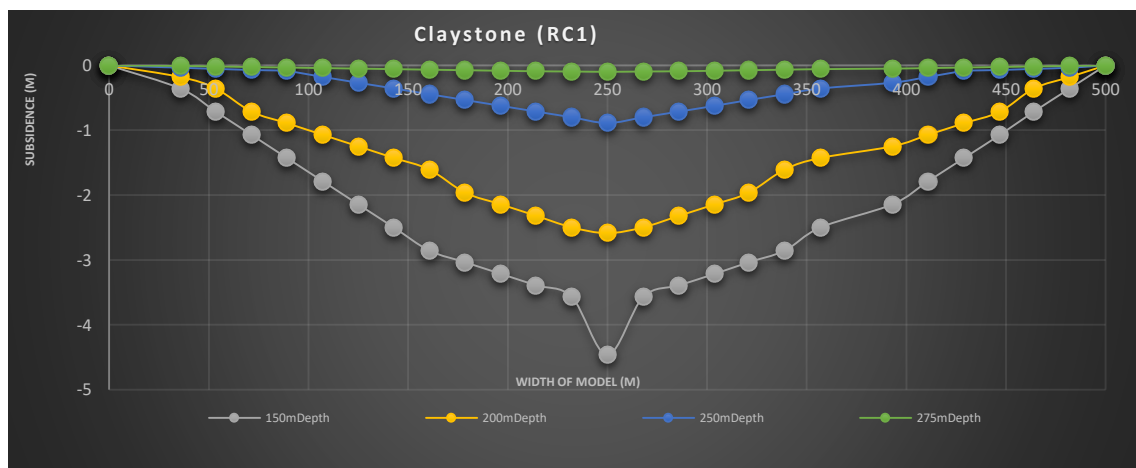


Figure 15. Graphics of surface subsidence at each depths

Table 8. Maximum subsidence for each rock types at each depth

Rock types	Subsidence (m)			
	150 m depth	200 m depth	250 m depth	275 m depth
RC1	-4.46	-2.59	-0.89	-0.10
RC2	-7.23	-4.19	-1.44	-0.16
RS1	-4.88	-2.83	-0.98	-0.11
RS2	-6.10	-3.54	-1.22	-0.14
RSS2	-6.95	-4.03	-1.39	-0.16
Max. Subsidence	-7.23	-4.19	-1.44	-0.16
Min. Subsidence	-4.46	-2.59	-0.89	-0.10

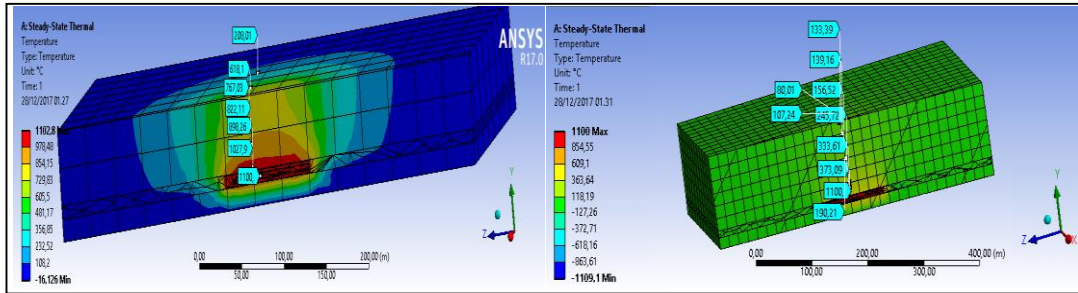


Figure 16. Temperature variation from thermal source to surface at 50 and 100m depth

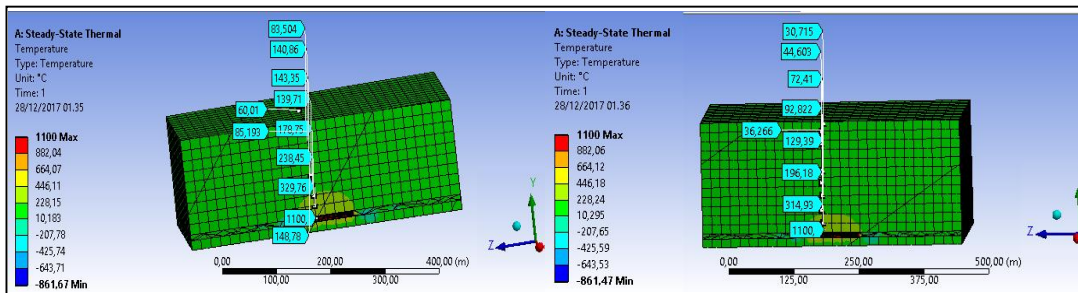


Figure 17. Temperature variation from thermal source to surface at 150 and 200m depth

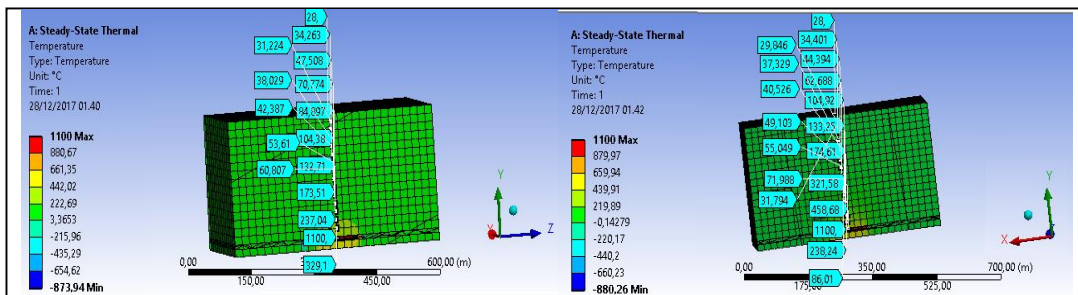


Figure 18. Temperature variation from thermal source to surface at 250 and 275 m depth

Table 10 is a summary of the maximum temperature conditions at each depth. These results indicate that in general the temperature on the surface will begin to

stabilize and be safe for living things if the gasifier is at a depth of > 200m from the surface.

Table 10. Summary of temperature conditions at each depth

Rock types	Temperatures (°C) at each depth					
	50m	100m	150m	200m	250m	275m
RC1	208	80	60	29	28	28
RC2	278	132	72	31	28	28
RS1	213	93	69	30	28	28
RS2	268	134	72	31	28	28
RSS2	289	133	74	32	28	28
Max. Temp.	289	134	74	32	28	28
Min. Temp.	213	93	69	29	28	28

## CONCLUSION AND SUGGESTION

### Conclusion

Numerical modeling is useful to determine the rock thickness that safe above the coal seam, avoid the surface subsidence, and prevent the influence of high temperature from UCG process. The modelling result of this study shows that the rock thickness above 150 m from the UCG coal seam at the location is still prone to surface subsidence, although in some rock types at more shallow from the 150 m are still safe shown by the safety factor  $> 1$ .

From the results of this modeling, the depth more above 200 m at the study location is quite safe with the smallest SF 1.59. If the thickness of cap rock 150 m, the maximum of surface subsidence occurs -7.23 m for the type of non-kaolinite claystone and the smallest occurs -0.10 m for the type of kaolinite claystone at 275 m depth.

To reduce the surface subsidence, it is necessary to regulate the gasification process by leaving some coals as a pillar, unless there is no infrastructure on the surface that can be disturbed due to the UCG process. When viewed from the results of the heat propagation modeling results from the cavity of the gasifier to the surfaces, at a depth of 50m, the surface temperature is still around 213-289°C but above 200 m depth from the surface is a safe condition for humans and other living things.

### Suggestion

For the modeling results to be more in line with the actual conditions, a more detailed test of the thermal properties of high-temperature rocks, especially the specific heat ( $C_p$ ), thermal conductivity ( $\lambda$ ), thermal expansion coefficient ( $\alpha$ ) and thermal diffusivity is needed in further research. Besides, it is necessary to have a triaxial creep test on rocks that have been subjected to thermal loads with sufficient confining pressure variations.

## ACKNOWLEDGEMENT

I would like to express my deepest gratitude to the R&D Center for Mineral and Coal Technology (*teKMIRA*), Agency of R&D Energy and Mineral Resources-ESDM for

providing the opportunity to the author to conduct this research. Support from friends in the geo-mechanics laboratory-*teKMIRA* gave encouragement to complete this research.

## REFERENCES

- Advani, S. H., Lee, J. K., Min, O. K., Aboustite, B. L., Chen, S. M. and Lee, S. C. (1983) "Stress mediated responses associated with UCG cavity and subsidence prediction modeling," in Wieber, P. R., Martin, J. W., and Byrer, C. W. (eds.) *Proceedings of the Ninth Annual Underground Coal Gasification Symposium*. Bloomington, Illinois: L B Schaeffer EC&G, Washington Analytical Services Center Inc., Morgantown Operations, pp. 282–292.
- Asadi, A., Shahriar, K., Goshtasbi, K. and Najm, K. (2005) "Development of a new mathematical model for prediction of surface subsidence due to inclined coal-seam mining," *Journal of The South African Institute of Mining and Metallurgy*, 105(1), pp. 15–20.
- Boldyrev, G. G. and Muyzemnek, A. J. (2008) "The modeling of deformation process in soils with use of ansys and Ls-Dyna programs," in *6th International Conference on Case Histories in Geotechnical Engineering*. Missouri University of Science and Technology, pp. 1.08 (1-10).
- Christensen, R. M. (2019) *Failure theory for materials science and engineering: Chapter VII-The ductile/brittle transition, gaging ductility levels*, [www.failurecriteria.com](http://www.failurecriteria.com). Available at: [https://www.failurecriteria.com/Media/Ductile\\_Brittle\\_Transition\\_Gaging\\_Ductility\\_Level.pdf](https://www.failurecriteria.com/Media/Ductile_Brittle_Transition_Gaging_Ductility_Level.pdf) (Accessed: August 25, 2020).
- Dong, S., Yin, H., Yao, S. and Zhang, F. (2013) "Detecting surface subsidence in coal mining area based on DInSAR technique," *Journal of Earth Science*, 24(3), pp. 449–456. doi: 10.1007/s12583-013-0342-1.
- Drucker, D. C. and Prager, W. (1952) "Soil mechanics and plastic analysis or limit design," *Quarterly of Applied Mathematics*, 10(2), pp. 157–165.
- Dyne, L. A. (1998) *The prediction and occurrence of chimney subsidence in Southwestern Pennsylvania*. Virginia Polytechnic Institute and State University. Available at: <https://techworks.lib.vt.edu/handle/10919/31383>.

- Ellison, R. D. and Schubert, C. E. (1981) "Subsidence effects guidelines for underground coal gasification," in *7th underground coal conversion symposium*. Fallen Leaf Lake, California: OSTI.GOV, pp. 799–822. doi: 10.1002/1097-0207(20000730)48:9<1285::AID-NME825>3.0.CO;2-H.
- Eppelbaum, L., Kutasov, I. and Pilchin, A. (2014) *Applied geothermics*. Berlin, Heidelberg: Springer Berlin Heidelberg (Lecture Notes in Earth System Sciences). doi: 10.1007/978-3-642-34023-9.
- Gregg, D. W. (1977) *Ground subsidence resulting from underground coal gasification*. Livermore, CA.
- Huayang, D., Jinzhuang, W., Meifeng, C., Lixin, W. and Zengzhang, G. (2002) "Seam dip angle based mining subsidence model and its application," *International Journal of Rock Mechanics and Mining Sciences*, 39(1), pp. 115–123. doi: 10.1016/S1365-1609(02)00008-4.
- Irsyam, M., Sengara, W., Aldiamar, F., Widiyantoro, S., Triyos, W., Hilman, D., Kertapati, E., Meilano, I., Suhardjono, Asrurifak, M. and Ridwan, M. (2010) *Ringkasan hasil studi tim revisi peta gempa Indonesia 2010*. Bandung: Tim Revisi Peta Gempa Indonesia.
- Langland, R. T. and Trent, B. C. (1981) "Computer models to support investigations of surface subsidence and associated ground motion induced by underground coal gasification." Livermore: Lawrence Livermore National Lab., CA (USA); Science Applications, Inc., Steamboat Springs, CO (USA), UCRL-86437; CONF-810923-1.
- Lee, J. K., Avasthi, J. M., Advani, S. H. and Kitamura, M. (1985) "Parameter sensitivity studies for UCG related subsidence modeling," in *The 11th underground coal gasification symposium*. Denver, Colorado: OSTI.GOV, pp. 424–433.
- Lee, J. K., Advani, S. H., Chen, K. S. and Avasthi, J. M. (1986) "Application of rock mechanics and the finite element method to underground coal gasification process," in *The 27th U.S. Symposium on Rock Mechanics (USRMS)*. Tuscaloosa, Alabama: American Rock Mechanics Association.
- Li, S. and Liu, W. K. (2000) "Numerical simulations of strain localization in inelastic solids using mesh-free methods," *International Journal for Numerical Methods in Engineering*, 48(9), pp. 1285–1309. doi: 10.1002/1097-0207(20000730)48:9<1285::AID-NME825>3.0.CO;2-H.
- Min, O. K. (1983) *Finite element modeling of thermo-mechanical responses associated with underground coal conversion*. Ohio State University.
- Neto, E. A. de S., Peric, D. and Owen, D. R. J. (2008) *Computational methods for plasticity: Theory and applications*. Wiley.
- Otto, C. and Kempka, T. (2015) "Thermo-mechanical simulations of rock behavior in underground coal gasification show negligible impact of temperature-dependent parameters on permeability changes," *Energies*, 8(6), pp. 5800–5827. doi: 10.3390/en8065800.
- Pilkey, W. D. (1994) *Peterson's stress concentration factors*. John Wiley & Sons, Inc.
- Purnama, A. and Huda, M. (2019) "A preliminary study of Indonesian coal basins for underground coal gasification development," *Indonesian Mining Journal*, 22(1), pp. 61–76. doi: 10.30556/imj.Vol22.No1.2019.275.
- Seccombe, K. R. (2014) *Numerical modelling of mining subsidence*. University of Southern Queensland. Available at: [https://eprints.usq.edu.au/27315/1/Seccombe\\_2014.pdf](https://eprints.usq.edu.au/27315/1/Seccombe_2014.pdf).
- Sica, L. U. R. (2017) *An experimental study of the validity of the von Mises yielding criterion for elasto-viscoplastic materials*. Pontificia Universidade Católica. Available at: [https://www.researchgate.net/profile/Luiz\\_Umberto\\_Rodrigues\\_Sica2/publication/329150784\\_An\\_experimental\\_study\\_of\\_the\\_validity\\_of\\_the\\_von\\_Mises\\_yielding\\_criterion\\_for\\_elasto-viscoplastic\\_materials/links/5bf7f338a6fdcc53881530a3/An-experimental-study-of-the](https://www.researchgate.net/profile/Luiz_Umberto_Rodrigues_Sica2/publication/329150784_An_experimental_study_of_the_validity_of_the_von_Mises_yielding_criterion_for_elasto-viscoplastic_materials/links/5bf7f338a6fdcc53881530a3/An-experimental-study-of-the).
- Sirdesai, N. N., Singh, R., Singh, T. N. and Ranjith, P. G. (2015) "Numerical and experimental study of strata behavior and land subsidence in an underground coal gasification project," *Proceedings of the International Association of Hydrological Sciences*, 372, pp. 455–462. doi: 10.5194/piahs-372-455-2015.
- Siriwardane, H. J., Layne, A. W. and Martin, J. W. (1989) "Thermo-mechanical modeling of ground movements associated with large underground coal gasification cavities in

- thin coal seams," in *Delft University of Technology International Underground Coal Gasification Symposium*. Delft, Netherlands: Delft University of Technology, pp. 296–307.
- Sroka, A., Tajdus, K. and Preusse, A. (2011) "Calculation of subsidence for room and pillar and longwall panels," in Aziz, N. and Kininmonth, B. (eds.) *Proceedings of the 2011 Coal Operators' Conference*. University of Wollongong: University of Wollongong Australia, pp. 83–90.
- Sury, M., White, M., Kirton, J., Carr, P. and Woodbridge, R. (2004) *Review of environmental issues of underground coal gasification*. Birmingham.
- Szabó, L. and Kossa, A. (2012) "A new exact integration method for the Drucker–Prager elastoplastic model with linear isotropic hardening," *International Journal of Solids and Structures*, 49(1), pp. 170–190. doi: 10.1016/j.ijsolstr.2011.09.021.
- Tian, H., Kempka, T., Feinendegen, M., Schlüter, R. and Ziegler, M. (2009) "Influence of high temperature on rock mass surrounding in situ coal conversion sites," in *10th International Symposium on Environmental Geotechnology and Sustainable*. Bochum, Germany, pp. 128–132.
- Tian, H., Kempka, T., Xu, N.-X. and Ziegler, M. (2012) "Physical properties of sandstones after high temperature treatment," *Rock Mechanics and Rock Engineering*, 45(6), pp. 1113–1117. doi: 10.1007/s00603-012-0228-z.
- Tian, H. (2013) *Development of a thermo-mechanical model for rocks exposed to high temperatures during underground coal gasification*. Rheinisch-Westfälischen Technischen Hochschule Aachen. Available at: <https://d-nb.info/1035674211/34>.
- Tian, H., Kempka, T., Yu, S. and Ziegler, M. (2016) "Mechanical properties of sandstones exposed to high temperature," *Rock Mechanics and Rock Engineering*, 49(1), pp. 321–327. doi: 10.1007/s00603-015-0724-z.
- Tian, H., Ziegler, M. and Kempka, T. (2011) "Mechanical behavior of claystone exposed to high temperatures and its possible impacts on the stability of a deep nuclear waste repository," in Cai, M. (ed.) *Rock Mechanics: Achievements and Ambitions*. London, UK: CRC Press, pp. 193–197. doi: 10.1201/b11438-39.
- Tian, H., Ziegler, M. and Kempka, T. (2014) "Physical and mechanical behavior of claystone exposed to temperatures up to 1000 °C," *International Journal of Rock Mechanics and Mining Sciences*, 70, pp. 144–153. doi: 10.1016/j.ijrmms.2014.04.014.
- Turteltaub, S. (2002) "Inelastic analysis of structures, Milan Jirásek and Zdeněk P. Bažant, John Wiley & Sons, 2002, ISBN 0-471-98716-6, 758 Pages," *Structural and Multidisciplinary Optimization*, 24(1), pp. 87–88. doi: 10.1007/s00158-002-0217-z.
- Waddington, A. A. and Kay, D. R. (1995) "The incremental profile method for prediction of subsidence, tilt, curvature and strain over a series of panels," in *Mine Subsidence Technological Society, Third Triennial Conference on Buildings and Structures Subject to Ground Movement*. Newcastle: Mine Subsidence Engineering Consultants Pty Ltd, pp. 189–198.
- Walter, K. (2007) "Fire in the hole: Underground coal gasification may provide a secure energy supply and reduce greenhouse gas emissions," *Science & Technology Review*, April, pp. 12–18. Available at: <https://str.llnl.gov/content/pages/past-issues-pdfs/2007.04.pdf>.
- Whittaker, B. N. and Reddish, D. J. (1989) *Subsidence: Occurrence, prediction and control*. 1st ed. Elsevier Science.
- Zangerl, C. J. (2003) *Analysis of surface subsidence in crystalline rocks above the Gotthard highway tunnel, Switzerland*. Swiss Federal Institute of Technology (ETH) Zürich.
- Zulfahmi, Syafri, I., Abdurrokhim and Wattimena, R. K. (2017a) "Influence of mineral composition to rock strength on UCG process," *International Journal of Science and Research (IJSR)*, 6(6), pp. 1258–1262.
- Zulfahmi, Syafri, I., Abdurrokhim and Wattimena, R. K. (2017b) "Thermal effects of geomechanics characteristics of soft rocks from M. Enim formation," in *The 2017 World Congress on Advances in Structural Engineering and Mechanics (ASEM17)*. IIsan (Seoul), Korea: IASEM, p. YP.05.SM1105\_4395F6\_2.